Molecular Pharmacology Fast Forward. Published on April 4, 2011 as DOI: 10.1124/mol.110.070284
Molecular Pharmacology Fast Forward. Published on April 4, 2011 as DOI: 10.1124/mol.110.070284
This article has not been copyedited and formatted. The final version may differ from this version.
MOL #70284

Cyclopentenyl cytosine induces senescence in breast cancer cells through the nucleolar stress response and activation of p53

Min Huang, Patrick Whang, Patrick Lewicki, and Beverly S. Mitchell

From the Department of Medicine, Divisions of Oncology and Hematology, and the Stanford Cancer Center, Stanford University School of Medicine, Stanford, CA, 94305.

Downloaded from molpharm.aspetjournals.org at ASPET Journals on April 18, 2024

Copyright 2011 by the American Society for Pharmacology and Experimental Therapeutics.

Molecular Pharmacology Fast Forward. Published on April 4, 2011 as DOI: 10.1124/mol.110.070284
This article has not been copyedited and formatted. The final version may differ from this version.
MOL #70284

Running title: CTP depletion induces cellular senescence

Corresponding author: Beverly S. Mitchell**,** Stanford Cancer Center, LLSC Research Building (SIM1), 265 Campus Drive, Rm. 2167, Stanford, CA 94305-5458. Telephone: 650-725-9621. Fax: 650-736-0607, e-mail address: bmitchell@stanford.edu

Number of text pages: 16

Number of tables: 0

Number of figures: 7

Number of references: 45

Number of words in the abstract: 231

Number of words in the introduction: 510

Number of words in the discussion: 1103

Abbreviations list: CPEC, cyclopentenyl cytosine; ENT1, equilibrative nucleoside transporter 1; ENT2, equilibrative nucleoside transporter 2; EGFP-NS, EGFP-tagged nucleostemin; SA-*β*-gal, senescence-associate β-galactosidase activity; AraC, 1-β-D-arabinofuranosylcytosine; dFdC, 2',2'-difluorodeoxycytidine; DAPI, 4',6-diamino-2-phenylindol; PBS, phosphate-buffered saline; PI, propidium iodide; NPM1, nucleophosmin1; Pol I, RNA polymerase I; NS, nucleostemin; CDK, cyclin-dependent kinase

Downloaded from molpharm.aspetjournals.org at ASPET Journals on April 18, 2024

Molecular Pharmacology Fast Forward. Published on April 4, 2011 as DOI: 10.1124/mol.110.070284
This article has not been copyedited and formatted. The final version may differ from this version.

Abstract

The induction of senescence has emerged as a potentially important contributor to the effects of chemotherapeutic agents against tumors. We have demonstrated that depletion of CTP induced by cyclopentenyl cytosine (CPEC, NSC 375575), a specific inhibitor of the enzyme CTP synthetase, induces irreversible growth arrest and senescence characterized by altered morphology and expression of senescence-associated U+0392-galactosidase activity (SA-U+0392-gal) in MCF-7 breast cancer cells expressing wild type p53. In contrast, differentiation in the absence of senescence resulted from CPEC treatment in MDA-MB-231 breast cancer cells that express a mutated p53. Both senescence of MCF-7 cells and differentiation of MDA-MB-231 cells were prevented by repletion of CTP through the cytidine salvage pathway. Senescence in MCF-7 cells was associated with a G2 and S phase arrest, whereas differentiation in MDA-MB-231 cells was associated with arrest in G1 phase at 5 days. Mechanistic studies revealed that CTP depletion induced a rapid translocation of nucleolar proteins including nucleostemin and nucleolin into the nucleoplasm. This nucleolar stress response resulted in a sustained elevation of p53 and the p53 target genes, p21 and Mdm2, in cells with wild-type p53. Furthermore, siRNA-induced knockdown of p53 in MCF-7 cells treated with CPEC prevented cellular senescence and increased apoptotic cell death. We conclude that CTP depletion and the resulting nucleolar stress response results in a senescence-like growth arrest through activation of p53, while cells with mutated p53 undergo differentiation or apoptotic cell death.

Downloaded from molpharm.aspetjournals.org at ASPET Journals on April 18, 2024

Molecular Pharmacology Fast Forward. Published on April 4, 2011 as DOI: 10.1124/mol.110.070284
This article has not been copyedited and formatted. The final version may differ from this version.

Introduction:

Transformed cells retain the ability to undergo premature or replicative senescence in response to various stimuli. Senescent cells undergo irreversible cell cycle arrest and display characteristic phenotypic alterations, including an enlarged and flattened morphology and expression of senescence-associate β-galactosidase activity (SA-*β*-gal) (Dimri et al., 1995). Some anticancer agents induce a rapid, non-telomere-dependent form of senescence, often termed premature senescence, in cancer cells at concentrations that do not cause acute cell death *in vitro* or *in vivo* (Hornsby, 2007). These agents include PI-3 kinase inhibitors (Collado et al., 2000), retinoic acid (Roninson and Dokmanovic, 2003), microtubule-stabilizing agents (Arthur et al., 2007), Sirt1 (Ota et al., 2006) and DNA topoisomerase inhibitors (Michishita et al., 1998), doxorubicin (Vigneron et al., 2005) and cisplatin (Varna et al., 2009). Induction of SA- *β*-gal staining after chemotherapy has been observed in cells obtained from patients with breast cancer (te Poele et al., 2002) and senescence-like growth arrest has been proposed as a determinant of *in vivo* tumor response to both selective chemotherapeutic agents and ionizing radiation (Kahlem et al., 2004).

Multiple mechanisms have been implicated in the induction of senescence, including telomere shortening induced by inhibition of TERT activity (Kim et al., 2003), induction of p53 (reviewed in Ref (Chang et al., 1999)), increased expression of cyclin-dependent kinase inhibitors such as p16 INK4a (Uhrbom et al., 1997), p21 (Fang et al., 1999) and p27 (Collado et al., 2000), and dephosphorylation of Rb (Xu et al., 1997).

Cyclopentenyl cytosine (CPEC) is an analogue of cytidine (Kang et al., 1989) and enters cells preferentially through the equilibrative nucleoside transporters including ENT1 and ENT2 (Huang et al., 2004). Intracellularly, CPEC is metabolized into its mono-, di-, and triphosphate forms (Kang et al., 1989). In its triphosphate form, it serves as a specific

Downloaded from molpharm.aspetjournals.org at ASPET Journals on April 18, 2024

noncompetitive inhibitor of CTP synthetase, which catalyses the conversion of UTP to CTP as the predominant pathway for CTP synthesis in proliferating cells (Schimmel et al., 2007). As a result, the intracellular CTP pool is rapidly depleted (Huang et al., 2004; Kang et al., 1989). Previous studies have established the anti-tumor effects of CPEC using a number of tumor cell lines (Schimmel et al., 2007) and several tumor models (Schimmel et al., 2007; Van Bree et al., 2009) . In addition, CPEC was shown to act at nanomolar concentrations *in vitro* as a chemosensitizer to enhance the anti-cancer effects of several nucleoside analogues such as AraC (1-β-D-arabinofuranosylcytosine) and 2',2'-difluorodeoxycytidine (dFdC, gemcitabine) in a variety of tumor cell lines (Schimmel et al., 2007), although no enhanced efficacy of CPEC was found when combined with gemcitabine and radiation in two animal tumor models (Van Bree et al., 2009).

In the present study, we have found that CTP depletion results in a pronounced nucleolar stress response. The effects of CTP depletion on cell proliferation, differentiation, apoptosis, and cellular senescence and related signaling pathways were assessed. These data provide evidence that nucleolar stress triggered by CTP depletion serves to regulate critical events leading to the induction of senescence or differentiation/apoptosis depending on the p53 status of the cell.

Materials and methods:

Cell culture conditions and reagents used. The p53 wild-type MCF-7 human breast tumor cell line and p53 mutant MDA-MB-231 cells were obtained from ATCC. U2OS cells stably expressing EGFP-tagged NS (EGFP-NS) have been described previously (Huang et al., 2009). U2OS, MCF-7, and MDA-MB-231 cells were grown in Dulbecco's Modified Eagle (DMEM) medium supplemented with 10% fetal calf serum (HyClone; PERBIO), 1 mM sodium pyruvate, 0.1 mM non-essential amino acids, 100 U/ml of penicillin and

Downloaded from molpharm.aspetjournals.org at ASPET Journals on April 18, 2024

Molecular Pharmacology Fast Forward. Published on April 4, 2011 as DOI: 10.1124/mol.110.070284
This article has not been copyedited and formatted. The final version may differ from this version.

streptomycin at 37°C in a humidified, 5% CO_2 atmosphere. Nutlin-3 was obtained from EMD (EMD Chemicals, Inc., NJ, USA). 4',6-diamino-2-phenylindol (DAPI) was purchased from Molecular Probes, Inc (Eugene, OR, USA). Mouse monoclonal anti-nucleolin (MS-3) and anti-p53 (DO-1) were from Santa Cruz Biotechnology (Santa Cruz, CA, USA). Rabbit polyclonal anti-NPM was from Cell Signaling Technology Inc. (Beverly, MA, USA). Goat anti-nucleostemin polyclonal antibody was from R&D Systems (R&D Systems, Inc., MN, USA). Anti-actin monoclonal antibody was from Sigma (Sigma-Chemical Co., St. Louis. USA). Full-length A.v. polyclonal EGFP antibody was from Clontech Laboratories (Clontech Laboratories, Inc., CA, USA). Fluorescein (FITC)-conjugated donkey anti-rabbit F(ab')2 and rhodamine-conjugated goat anti-mouse secondary antibodies were purchased from Jackson ImmunoResearch (West Grove, PA, USA). siRNA SMARTpool against p53 was obtained from Dharmacon (Lafayette, CO, USA). CPEC was kindly provided by Dr. Lee Graves, the University of North Carolina at Chapel Hill.

Assay of senescence-associated β-galactosidase activity (SA- β -gal). SA- β -gal staining was performed as previously described (Dimri et al., 1995). At the appropriate times after treatment, cells were washed twice in PBS, fixed in 2% formaldehyde/0.2% glutaraldehyde for 5 min at room temperature, washed again in PBS, and incubated with *β*-galactosidase staining solution containing 1 mg/ml X-Gal (5-bromo-4-chloroindol-3-yl *β*-D-galactopyranoside), 40 mM citric acid/sodium phosphate, pH 6, 5 mM potassium ferrocyanide, 5 mM ferricyanide, 150 mM NaCl and 2 mM $MgCl_2$. Following overnight incubation at 37°C, cells were photographed. The extent of senescence was quantified based on the mean number of cells displaying both changes in morphology as well as percent blue-green staining in 8 fields that contained at least 50 cells per field for each experimental condition. All treatments were carried out in triplicate and results represent the mean +/- SD.

Downloaded from molpharm.aspetjournals.org at ASPET Journals on April 18, 2024

Molecular Pharmacology Fast Forward. Published on April 4, 2011 as DOI: 10.1124/mol.110.070284
This article has not been copyedited and formatted. The final version may differ from this version.

BrdU incorporation and Cell Cycle Analysis. Cells were incubated in medium containing DMSO or CPEC at the concentrations and times indicated. Cells were then incubated with 100 μM BrdU (Sigma) at 37°C for 2 hours before harvest. Approximately 1×10^6 cells were harvested with trypsin, washed in cold phosphate-buffered saline (PBS) and the pellets were resuspended and fixed with 70% ethanol at 4°C overnight. Cells were washed with PBS, resuspended in 1 ml of 2 N HCl supplemented with 0.5% Triton X-100 and incubated for 30 minutes at room temperature. After neutralizing the samples with 1 mL of 100 μM borate buffer (Na2B4O7, pH 8.5), the cells were washed with PBS followed by PBS containing 0.5% Tween 20 and 1% BSA. The cells were resuspended in 100 µl PBS containing 5 µl of FITC-conjugated anti-BrdU antibody (Caltag Laboratories, Burlingame, CA), 0.5% Tween 20, and 1% BSA, and incubated for overnight at 4°C. Cells were then washed with PBS containing 0.5% Tween 20, and 1% BSA, and resuspended in 0.5 ml PBS containing 5 µg/ml propidium iodide, 0.5% Tween 20, and 1% BSA, and incubated for 30 minutes at room temperature in the dark. Prior to analysis, each sample was filtered through a 35 µm nylon mesh. The percentage of cells in each phase of the cell cycle and the percentage of cells incorporating BrdU was assessed by dual color flow cytometric analyses using a FACScan (BectonDickinson) and analyzed using FlowJo© software. A minimum of 50,000 events were collected for each sample.

Immunocytochemistry. U2OS, U2OS cells stably expressing EGFP-NS, MCF-7 and MDA-MB-231 cells were grown on cover slips in 24-well plates in DMEM complete medium for 12 h, then treated with CPEC or vehicle control at the concentrations and times indicated. The cells were fixed in 4% phosphate-buffered saline (PBS)-paraformaldehyde solution for 20 min followed by permeabilization with 0.1% Triton X-100 in PBS for 15 min. After blocking with 5% bovine serum albumin in PBS for 30 min, cover slips were inverted onto a

Downloaded from molpharm.aspetjournals.org at ASPET Journals on April 18, 2024

Molecular Pharmacology Fast Forward. Published on April 4, 2011 as DOI: 10.1124/mol.110.070284
This article has not been copyedited and formatted. The final version may differ from this version.

30µl drop of the primary antibodies diluted in PBS containing 0.1% Triton-X-100 and 5% BSA (1:50 for nucleolin, Mdm2, and nucleostemin). After 1 h incubation with antibody and subsequent washing with PBS x 3 (10 min each), coverslips were inverted again onto 30µl drops of the secondary antibodies diluted in PBS containing 5% BSA and 0.1% Triton-X 100 (rhodamine-congugated secondary antibody (1:300); fluorescein isothiocyanate-conjugated secondary antibody (1:50)). After washing, cover slips were stained with DAPI (300 nM) for 5 minutes, and washed with PBS x 3 (5 min. each), mounted in Gel Mount IM Aqueous Mounting Medium (Sigma-Chemical Co., USA) and examined using fluorescent microscopy.

Western blotting. Immunoblot analysis was performed as previously described (Huang et al., 2009).

Apoptosis assay. Quantitation of apoptosis by annexin V/ propidium iodide (PI) staining was performed as described previously (Huang et al., 2002). Briefly, MCF-7 cells were transfected with p53 Smartpool siRNA (100 nM) and control siRNA (100 nM) by Amaxa Electroporation. 24 h after electroporation, cells were exposed to CPEC or DMSO vehicle control for 5 days. Apoptotic cell death was determined using the BD ApoAlert Annexin V–FITC Apoptosis Kit (BD Biosciences, USA) according to the manufacturer's instructions, and cells were analyzed using flow cytometry.

Oil Red staining. Cells grown in 12 well plates were washed with PBS, fixed with paraformaldehyde, washed three times with PBS, and stained with Oil Red O (Sigma Chemical) for 10 min according to published procedures (Ryden et al., 2003). Stained cells were then examined and photographed. The percentage of cells staining positive for lipid droplet accumulation was determined by counting the number of cells containing 10 or more Oil Red O-stained lipid droplets.

Silencing of endogenous p53 by small interfering RNAs (siRNA). siRNA SMART pool

Downloaded from molpharm.aspetjournals.org at ASPET Journals on April 18, 2024

targeting p53 and a scrambled control oligonucleotide (5'-AAAGTCATCGTGACTCGACG-3') were described previously (Huang et al., 2009). The oligonucleotides were electroporated into MCF-7 cells using the Amaxa Electroporation kit V (Amaxa) according to the manufacturer´s instruction. 2×10^6 cells/sample were resuspended in 100 µl Nucleofector ™ solution at room temperature and electroporated into MCF-7cells using 100 pmol or 200 pmol of SMART pool p53-siRNA, scrambled control-siRNA (Program P-20 for MCF-7 on the Amaxa Nucleofector Device). Twenty-four hours following electroporation of p53-siRNA, MCF-7 cells were exposed to 1 µM CPEC or vehicle control. Cells were either processed after 8 h of CPEC exposure for western blot analysis of p53, Mdm2, or p21 or were left for analysis of senescence after 5 days of CPEC exposure.

Statistical Analysis. Results of SA-β-gal were expressed as compared statistically between the control and CPEC treated results with the paired Student's *t*-test with mean ± SD. A p value of < 0.05 was considered statistically significant.

Results:

Differential effects of CPEC treatment on MCF-7 and MDA-MB-231 cells. The effect of CPEC on growth of MCF-7/MDA-MB-231 cells was monitored over a 5 day interval. CPEC treatment inhibited growth in both cell types. After 5 days, MCF-7 cells displayed striking morphological changes consistent with cellular senescence, including cell enlargement, flattening, and a decreased nucleo-cytoplasmic ratio, while vehicle treated control cells remained unchanged. MDA-MB-231 cells harboring mutant p53 exhibited similar morphologic changes after CPEC treatment (supplemental Fig. 1). We then asked whether the growth arrest phenotype was caused by an induction of senescence, quiescence, or terminal differentiation. As shown in Fig. 1A, CPEC treatment of MCF-7 cells significantly increased the percentage of SA-β-gal-positive cells ($P<0.001$) in a concentration-dependent manner

Downloaded from molpharm.aspetjournals.org at ASPET Journals on April 18, 2024

after 5 days (Fig. 1A, 1B). Nutlin-3a, an inhibitor of Mdm2, was used as a positive control (Fig. 1C). In contrast, no increase in SA-β-gal positivity over background was observed in MDA-MB-231 cells treated with either CPEC or Nutlin-3a (Fig. 1A, 1C). Next, we investigated whether the growth arrest found in MDA-MB-231 cells was attributable to either quiescence or differentiation. CPEC-treated MDA-MB-231 cells were stained with oil-red to assay for lipid droplets as a reflection of differentiation of breast cancer cells (Adan et al., 2003). As shown in Fig. 2A, over 80% of MDA-MB-231 cells exhibited a marked increase in the presence of lipid droplets after 5 days of CPEC treatments, whereas MCF-7 cells did not stain with oil-red (Fig. 1). The addition of cytidine, previously shown to replenish intracellular CTP pools through its phosphorylation to CMP via uridine/cytidine kinase (Huang et al., 2004), almost completely prevented both the differentiation of MDA-MB-231 cells (Fig. 2A) and the senescence of MCF-7 cells (Fig. 2B) due to CPEC treatment. Collectively, these results indicate that the induction of senescence or differentiation in MCF-7 and MDA-MB-231 cells, respectively, is dependent on CTP depletion.

CPEC treatment differentially affects cell cycle progression in MCF-7 and MDA-MB-231 cells. To further analyze the mechanisms underlying growth arrest induced by CTP depletion, the effects of CPEC on tumor cell proliferation and cell cycle progression were examined using BrdU incorporation and flow cytometric analysis. Treatment with CPEC for 48 h initially increased the number of S-phase cells by about 2-fold for both MCF-7 (35.4-44.2.0 % versus 24.6 % for the control sample) (supplemental Fig. 2A) and MDA-MB-231 cells (40.7-49.5% versus 18.4 % for the control sample) (supplemental Fig. 3A) while decreasing the extent of BrdU incorporation into DNA (supplemental Fig. 2B and 3B). Despite the induction of an increase in the S-phase cell population in both cell lines at 48 h, 5 days of CPEC treatment resulted in cell cycle arrest in both the S and G2 phases in MCF-7

Downloaded from molpharm.aspetjournals.org at ASPET Journals on April 18, 2024

cells (Fig. 3A and 3B), but only in G1 in MDA-MB-231 cells (Fig. 4A and 4B). Nutlin-3a induced both a G1 and a G2 arrest in MCF-7 cells (Fig. 3A and 3B). In both cell lines, a sustained reduction in BrdU incorporation (from 37.5% to 12.8%-23.7% in MCF-7 cells and from 20.2% to 2.9-11.1% in MDA-MB-231 cells) was observed after 5 days after CPEC treatment (Fig. 3B, 4B), correlating with the lack of proliferation at this time point.

Effect of CPEC on activation of p53, p21, and γ-H2AX. It has been well established that downstream targets of p53 are able to trigger replicative/premature senescence (Collado et al., 2007). p21 (Waf1/Cip1) is a potent cyclin-dependent kinase inhibitor that is transcriptionally regulated by p53 and appears to be central to both p53-dependent (Collado et al., 2007) and p53-independent (Fang et al., 1999) senescence. In MCF-7 cells, CPEC treatment resulted in a sustained increase in both p53 and p21 expression. In addition, the expression of Mdm2, another p53 target, was induced by CPEC treatment in MCF-7 cells (Fig. 5A) while *β*-actin expression remained constant. A moderate increase in the Mdm2 protein level was also detected in p53-mutant MDA-MB-231 cells, suggesting there may be a p53 independent regulation of Mdm2 (Fig. 5B). The levels of p21 were unchanged in these cells (Fig. 5B). As expected, a similar pattern of p53 and Mdm2 accumulation was observed in nutlin3 treated MCF-7 cells (supplemental Fig. 4). Phosphorylated γ-H2AX, an indicator of DNA damage response, increased dramatically in MDA-MB-231 cells after 24 h of CPEC exposure, but did not change significantly in comparison to control in MCF-7 cells (Fig. 5A and 5B).

Role of p53 in CPEC-induced senescence. To further confirm the role of p53 in mediating CPEC-induced senescence, we used a Smart pool p53 siRNA that specifically depletes p53 protein expression and asked whether the knockdown of p53 would prevent CPEC-induced senescence. As shown in Fig. 6A, transfection of 200 pmol Smart pool siRNA of p53

Downloaded from molpharm.aspetjournals.org at ASPET Journals on April 18, 2024

reduced the level of endogenous p53 protein by well over 80%. Depletion of p53 using the siRNA approach completely prevented CPEC-induced elevation of Mdm2, (Fig. 6A) and significantly reduced the degree of senescence (P<0.001) (Fig. 6B and 6C), while increasing the percentage of Annexin V and PI double positive staining cells from 21.7 to 36.0% (Fig. 6D). An increased percentage of Annexin V and PI double positive staining cells (73.5%-77.9% of cells) suggestive of apoptosis was also observed in p53-null HL60 cells after exposure to CPEC at concentrations as low as 0.125 μM for 32 h (Fig. 6E). To further determine whether cell death was due to apoptosis, DNA was isolated from control or CPEC-treated cells and separated by agarose gel electrophoresis. As shown in Supplemental Fig. 5A, DNA fragmentation characteristic of apoptosis occurred in CPEC-treated p53-deficient HL60 cells. Similarly, enhanced DNA ladder formation was observed in CPEC-treated p53-depleted MCF-7 cells as compared with control MCF-7 cells (Supplemental Fig. 5B). These results indicate that p53 is central to CPEC-induced senescence of MCF-7 cells and that depletion of CTP by CPEC induces apoptotic cell death in the absence of p53.

Effect of CPEC on the localization of nucleolar proteins. Nucleolar disruption caused by inducers of nucleolar stress including inhibition of RNA polymerase I (Pol I) is implicated in the stabilization of p53 (Yuan et al., 2005). We have found previously that depletion of the cellular GTP pool by AVN-944 resulted in inhibition of pre-rRNA synthesis, disruption of nucleolar integrity, and stabilization of p53 (Huang et al., 2008). We therefore asked if CTP depletion induced similar disruption of nucleolar integrity that might serve as an up-stream signal resulting in p53 stabilization. Indeed, CTP depletion caused the rapid translocation of the nucleolar shuttle protein nucleostemin (NS) from the nucleolus to the nucleus and a moderate increase in Mdm2 protein expression in MCF-7 (Fig. 7A) and MDA-MB-231 cells (Fig. 7B). Because of their superior nucleolar morphology, we also used U2OS cells to evaluate the localization of nucleolar proteins. CPEC induced nucleoplasmic translocation of

Downloaded from molpharm.aspetjournals.org at ASPET Journals on April 18, 2024

Molecular Pharmacology Fast Forward. Published on April 4, 2011 as DOI: 10.1124/mol.110.070284
This article has not been copyedited and formatted. The final version may differ from this version.

NS and nucleolin in this cell line as well (Fig. 7C, Supplemental Fig. 6). Previous data have demonstrated that inhibition of Pol I by actinomycin D results in translocation of nucleolar PAF53 and TIF-IA, two components of the Pol I complex, to the nucleolar caps (Huang et al., 2008), a phenomenon reflecting "nucleolar stress". CTP depletion also induces similar translocation of TIF-IA and PAF53 from the nucleolus to the nucleolar caps (Supplemental Fig. 6), further supporting its inhibitory effect on Pol I activity through CTP depletion.

Discussion:

p53 is a central mediator of senescence in response to a variety of stress stimuli including DNA damage, oncogene over-expression, telomere dysfunction, and oxidative damage, as reviewed in (Collado et al., 2007). Our finding that CPEC induces senescence in MCF-7 cells expressing wild-type p53 in conjunction with sustained increases in p53 and p53-dependent Mdm2 and p21 expression while senescence is prevented by p53 depletion strongly implicates p53 accumulation as a prerequisite for the senescent phenotype.

Mdm2 maintains p53 at low levels by actively controlling its nuclear export (Freedman and Levine, 1998), transactivation (Momand et al., 1992), ubiquitination and proteosome-dependent degradation (Honda et al., 1997), and translation (Ofir-Rosenfeld et al., 2008). The Mdm2 gene is also a transcriptional target of p53 and an increase in p53 expression upon stress leads to activation of Mdm2 transcription (Barak et al., 1993). This Mdm2-p53 autoregulatory loop normally maintains p53 at low levels in non-stressed cells. Our evidence that depletion of cellular CTP leads to stabilization of wild-type p53 in the presence of excessive Mdm2 suggests that the inhibitory regulation of p53 by Mdm2 might be disrupted by CTP depletion. Several Mdm2-binding proteins have been shown to interfere with this autoregulatory loop through direct binding to the central acidic domain of Mdm2, thus inhibiting its E3 ubiquitin ligase activity and increasing p53 levels. These Mdm2-binding

Downloaded from molpharm.aspetjournals.org at ASPET Journals on April 18, 2024

proteins include ARF (Bothner et al., 2001), the ribosomal large-subunit proteins L5, L11, L23 (Lindstrom et al., 2007), the nucleolar protein nucleostemin (Dai et al., 2008; Meng et al., 2008) and very recently, the ribosomal small subunit protein 7 (S7) (Zhu et al., 2009). Of interest, most of those Mdm2 binding proteins are localized predominantly in the nucleolus under physiologic conditions, but are released from nucleolus into nucleoplasm in response to various stressors, including agents such as low dose actinomycin D that inhibit Pol I. We have previously shown that depletion of GTP induced by inhibition of its *de novo* synthetic pathway similarly induces a nucleolar stress response (Huang et al., 2008). In the present study, CPEC-mediated CTP depletion also results in nucleolar stress, causing nucleoplasmic translocation of nucleostemin and other nucleolar proteins including nucleolin and NPM1 and a simultaneous translocation of TIF-IA and PAF53, two components of the Pol 1 complex, to the nucleolar caps. Segregation of Pol I components into these fibrillar caps is a characteristic feature of inhibition of RNA Polymerase I-mediated transcription (Shav-Tal et al., 2005). It is reasonable to conclude that the release of nucleolar Mdm2-binding proteins triggered by CTP depletion is, at least in part, responsible for the increased stability of p53. The lack of ARF expression in MCF-7 cells rules out a role for ARF in the observed p53 activation (Della Ragione et al., 1995). However, the presumed release of other Mdm2-binding proteins including a number of small ribosomal subunit proteins is very likely to have played a role.

Cells entering senescence undergo irreversible cell cycle arrest, most often in the G1/S and/or G2/M phases of the cell cycle (Sugrue et al., 1997). Inducible expression of wild-type p53 in EJ bladder carcinoma cells, which have lost functional p53, was shown to trigger the rapid onset of G1 and G2/M senescent growth arrest associated with p21 up-regulation (Sugrue et al., 1997). Supporting a role for p53 in mediating G2 cell cycle arrest, nutlin-3a and CPEC both induce p53 accumulation and G2 arrest in MCF-7 cells that undergo

Downloaded from molpharm.aspetjournals.org at ASPET Journals on April 18, 2024

senescence (Fig 3A, 3B, and supplemental Fig. 4), but not in MDA-MB-231 cells expressing mutated p53 (Fig 4A and 4B). $p16^{INK4a}$ can also initiate senescence through inhibiting the cyclin-dependent kinases cdk4 and cdk6 (Uhrbom et al., 1997). However, MCF-7 and MDA-MB-231 cells both have homozygous deletions of $p16^{INK4}$ (Della Ragione et al., 1995), ruling out involvement of this protein as an effector of CPEC-induced senescence or differentiation. The increase in p-H2AX caused by CPEC treatment in MDA-MB-231 cells reflects a DNA damage response, most likely due to concomitant depletion of the cytidine deoxyribonucleotide pool. Under similar conditions, other deoxyribonucleotides are misincorporated into DNA, resulting in a similar DNA damage response (Schimmel et al., 2007).

The observation that depletion of endogenous p53 switched the cell fate of MCF-7 cells from a senescent to an apoptotic fate indicates that activation of the p53 pathway plays an essential role in inducing the senescence phenotype. It has been well documented that p53 mutations such as R175H, R273H, V135A mediate resistance to drug-induced apoptosis through suppression of procaspase-3 and caspase-3 (Lotem and Sachs, 1995; Tsang et al., 2005; Wong et al., 2007). These data raise the possibility that the expression of mutated p53 primes MDA-MB-231 cells for differentiation in response to nucleolar stress induced by CTP depletion, whereas p53 deficiency primes cells for apoptosis.

Although CPEC alone has established anti-tumor effects in a variety of cancer model systems, both *in vitro* and *in vivo* (Schimmel et al., 2007; Van Bree et al., 2009), severe cardiovascular toxicity was observed in five of 26 patients with solid tumors treated in a phase I clinical trial. However, this toxicity occurred only at the highest doses administered with corresponding steady-state plasma CPEC concentrations varying between 1.8-2.75 μM (Politi et al., 1995). Our data, in conjunction with those of others (Huang et al., 2004;

Downloaded from molpharm.aspetjournals.org at ASPET Journals on April 18, 2024

Schimmel et al., 2007), indicate that CPEC induces senescence, differentiation, or apoptosis at nanomolar concentrations in tumor cell lines *in vitro*. In theory, the effects of CPEC against tumors could be mitigated by cytidine present in human plasma. However, the physiological concentrations of uridine (5 µM) or cytidine (0.5 µM) in human plasma are not sufficient to prevent cell cycle arrest induced by nanomolar concentration of CPEC (50 nM) (Huang et al., 2004). In contrast to transformed cells, primary MEF cells expressing wild-type p53 are relatively resistant to CPEC treatment at concentrations up to 1µM (data not shown). It is quite possible that CPEC is selectively toxic to transformed cells due to increased uptake as the result of the increase in nucleoside transporters identified in tumor cells (Rauchwerger et al., 2000). Whether the intracellular metabolism of CPEC to its triphosphate form is also enhanced in some tumor cells through an increase in uridine-cytidine kinase activity (Kang et al., 1989) or a decrease in nucleotidase activity has not been investigated. If CPEC is to be reconsidered as an antineoplastic agent, especially given evidence of activity in p53-deficient cells, it will be important to investigate its relative uptake and metabolism in both tumor and normal tissue. A clinical resurgence of this drug would also require *in vitro* and *in vivo* studies to determine the optimal plasma concentration of CPEC that results in selective toxicity for tumor cells.

Authorship contributions: Participated in research design: Mitchell and Huang. Conducted experiments: Huang, Whang, Lewicki. Performed data analysis: Huang, Whang, Lewicki. Wrote or contributed to the writing of the manuscript: Huang and Mitchell. Other: Mitchell. acquired funding for the research.

Downloaded from molpharm.aspetjournals.org at ASPET Journals on April 18, 2024

References

Adan Y, Goldman Y, Haimovitz R, Mammon K, Eilon T, Tal S, Tene A, Karmel Y and Shinitzky M (2003) Phenotypic differentiation of human breast cancer cells by 1,3 cyclic propanediol phosphate. *Cancer Lett* **194**(1):67-79.

Arthur CR, Gupton JT, Kellogg GE, Yeudall WA, Cabot MC, Newsham IF and Gewirtz DA (2007) Autophagic cell death, polyploidy and senescence induced in breast tumor cells by the substituted pyrrole JG-03-14, a novel microtubule poison. *Biochem Pharmacol* **74**(7):981-991.

Barak Y, Juven T, Haffner R and Oren M (1993) mdm2 expression is induced by wild type p53 activity. *Embo J* **12**(2):461-468.

Bothner B, Lewis WS, DiGiammarino EL, Weber JD, Bothner SJ and Kriwacki RW (2001) Defining the molecular basis of Arf and Hdm2 interactions. *J Mol Biol* **314**(2):263-277.

Chang BD, Xuan Y, Broude EV, Zhu H, Schott B, Fang J and Roninson IB (1999) Role of p53 and p21waf1/cip1 in senescence-like terminal proliferation arrest induced in human tumor cells by chemotherapeutic drugs. *Oncogene* **18**(34):4808-4818.

Collado M, Blasco MA and Serrano M (2007) Cellular senescence in cancer and aging. *Cell* **130**(2):223-233.

Collado M, Medema RH, Garcia-Cao I, Dubuisson ML, Barradas M, Glassford J, Rivas C, Burgering BM, Serrano M and Lam EW (2000) Inhibition of the phosphoinositide 3-kinase pathway induces a senescence-like arrest mediated by p27Kip1. *J Biol Chem* **275**(29):21960-21968.

Dai MS, Sun XX and Lu H (2008) Aberrant expression of nucleostemin activates p53 and induces cell cycle arrest via inhibition of MDM2. *Mol Cell Biol* **28**(13):4365-4376.

Della Ragione F, Russo G, Oliva A, Mastropietro S, Mancini A, Borrelli A, Casero RA, Iolascon A and Zappia V (1995) 5'-Deoxy-5'-methylthioadenosine phosphorylase and p16INK4 deficiency in multiple tumor cell lines. *Oncogene* **10**(5):827-833.

Dimri GP, Lee X, Basile G, Acosta M, Scott G, Roskelley C, Medrano EE, Linskens M, Rubelj I, Pereira-Smith O and et al. (1995) A biomarker that identifies senescent human cells in culture and in aging skin in vivo. *Proc Natl Acad Sci U S A* **92**(20):9363-9367.

Fang L, Igarashi M, Leung J, Sugrue MM, Lee SW and Aaronson SA (1999) p21Waf1/Cip1/Sdi1 induces permanent growth arrest with markers of replicative senescence in human tumor cells lacking functional p53. *Oncogene* **18**(18):2789-2797.

Freedman DA and Levine AJ (1998) Nuclear export is required for degradation of endogenous p53 by MDM2 and human papillomavirus E6. *Mol Cell Biol* **18**(12):7288-7293.

Honda R, Tanaka H and Yasuda H (1997) Oncoprotein MDM2 is a ubiquitin ligase E3 for tumor suppressor p53. *FEBS Lett* **420**(1):25-27.

Hornsby PJ (2007) Senescence as an anticancer mechanism. *J Clin Oncol* **25**(14):1852-1857.

Huang M, Itahana K, Zhang Y and Mitchell BS (2009) Depletion of guanine nucleotides leads to the Mdm2-dependent proteasomal degradation of nucleostemin. *Cancer Res* **69**(7):3004-3012.

Huang M, Ji Y, Itahana K, Zhang Y and Mitchell B (2008) Guanine nucleotide depletion inhibits pre-ribosomal RNA synthesis and causes nucleolar disruption. *Leuk Res* **32**(1):131-141.

Huang M, Kozlowski P, Collins M, Wang Y, Haystead TA and Graves LM (2002) Caspase-

Downloaded from molpharm.aspetjournals.org at ASPET Journals on April 18, 2024

dependent cleavage of carbamoyl phosphate synthetase II during apoptosis. *Mol Pharmacol* **61**(3):569-577.

Huang M, Wang Y, Collins M and Graves LM (2004) CPEC induces erythroid differentiation of human myeloid leukemia K562 cells through CTP depletion and p38 MAP kinase. *Leukemia* **18**(11):1857-1863.

Kahlem P, Dorken B and Schmitt CA (2004) Cellular senescence in cancer treatment: friend or foe? *J Clin Invest* **113**(2):169-174.

Kang GJ, Cooney DA, Moyer JD, Kelley JA, Kim HY, Marquez VE and Johns DG (1989) Cyclopentenylcytosine triphosphate. Formation and inhibition of CTP synthetase. *J Biol Chem* **264**(2):713-718.

Kim JH, Lee GE, Kim SW and Chung IK (2003) Identification of a quinoxaline derivative that is a potent telomerase inhibitor leading to cellular senescence of human cancer cells. *Biochem J* **373**(Pt 2):523-529.

Lindstrom MS, Deisenroth C and Zhang Y (2007) Putting a finger on growth surveillance: insight into MDM2 zinc finger-ribosomal protein interactions. *Cell Cycle* **6**(4):434-437.

Lotem J and Sachs L (1995) A mutant p53 antagonizes the deregulated c-myc-mediated enhancement of apoptosis and decrease in leukemogenicity. *Proc Natl Acad Sci U S A* **92**(21):9672-9676.

Meng L, Lin T and Tsai RY (2008) Nucleoplasmic mobilization of nucleostemin stabilizes MDM2 and promotes G2-M progression and cell survival. *J Cell Sci* **121**(Pt 24):4037-4046.

Michishita E, Nakabayashi K, Ogino H, Suzuki T, Fujii M and Ayusawa D (1998) DNA topoisomerase inhibitors induce reversible senescence in normal human fibroblasts. *Biochem Biophys Res Commun* **253**(3):667-671.

Momand J, Zambetti GP, Olson DC, George D and Levine AJ (1992) The mdm-2 oncogene product forms a complex with the p53 protein and inhibits p53-mediated transactivation. *Cell* **69**(7):1237-1245.

Ofir-Rosenfeld Y, Boggs K, Michael D, Kastan MB and Oren M (2008) Mdm2 regulates p53 mRNA translation through inhibitory interactions with ribosomal protein L26. *Mol Cell* **32**(2):180-189.

Ota H, Tokunaga E, Chang K, Hikasa M, Iijima K, Eto M, Kozaki K, Akishita M, Ouchi Y and Kaneki M (2006) Sirt1 inhibitor, Sirtinol, induces senescence-like growth arrest with attenuated Ras-MAPK signaling in human cancer cells. *Oncogene* **25**(2):176-185.

Politi PM, Xie F, Dahut W, Ford H, Jr., Kelley JA, Bastian A, Setser A, Allegra CJ, Chen AP, Hamilton JM and et al. (1995) Phase I clinical trial of continuous infusion cyclopentenyl cytosine. *Cancer Chemother Pharmacol* **36**(6):513-523.

Rauchwerger DR, Firby PS, Hedley DW and Moore MJ (2000) Equilibrative-sensitive nucleoside transporter and its role in gemcitabine sensitivity. *Cancer Res* **60**(21):6075-6079.

Roninson IB and Dokmanovic M (2003) Induction of senescence-associated growth inhibitors in the tumor-suppressive function of retinoids. *J Cell Biochem* **88**(1):83-94.

Ryden M, Dicker A, Gotherstrom C, Astrom G, Tammik C, Arner P and Le Blanc K (2003) Functional characterization of human mesenchymal stem cell-derived adipocytes. *Biochem Biophys Res Commun* **311**(2):391-397.

Schimmel KJ, Gelderblom H and Guchelaar HJ (2007) Cyclopentenyl cytosine (CPEC): an overview of its in vitro and in vivo activity. *Curr Cancer Drug Targets* **7**(5):504-509.

Shav-Tal Y, Blechman J, Darzacq X, Montagna C, Dye BT, Patton JG, Singer RH and Zipori

Downloaded from molpharm.aspetjournals.org at ASPET Journals on April 18, 2024

D (2005) Dynamic sorting of nuclear components into distinct nucleolar caps during transcriptional inhibition. *Mol Biol Cell* **16**(5):2395-2413.

Sugrue MM, Shin DY, Lee SW and Aaronson SA (1997) Wild-type p53 triggers a rapid senescence program in human tumor cells lacking functional p53. *Proc Natl Acad Sci U S A* **94**(18):9648-9653.

te Poele RH, Okorokov AL, Jardine L, Cummings J and Joel SP (2002) DNA damage is able to induce senescence in tumor cells in vitro and in vivo. *Cancer Res* **62**(6):1876-1883.

Tsang WP, Ho FY, Fung KP, Kong SK and Kwok TT (2005) p53-R175H mutant gains new function in regulation of doxorubicin-induced apoptosis. *Int J Cancer* **114**(3):331-336.

Uhrbom L, Nister M and Westermark B (1997) Induction of senescence in human malignant glioma cells by p16INK4A. *Oncogene* **15**(5):505-514.

Van Bree C, Barten-Van Rijbroek AD, Leen R, Rodermond HM, Van Kuilenburg AB and Kal HB (2009) Cyclopentenyl cytosine has biological and anti-tumour activity, but does not enhance the efficacy of gemcitabine and radiation in two animal tumour models. *Int J Oncol* **34**(3):813-819.

Varna M, Lehmann-Che J, Turpin E, Marangoni E, El-Bouchtaoui M, Jeanne M, Grigoriu C, Ratajczak P, Leboeuf C, Plassa LF, Ferreira I, Poupon MF, Janin A, de The H and Bertheau P (2009) p53 dependent cell-cycle arrest triggered by chemotherapy in xenografted breast tumors. *Int J Cancer* **124**(4):991-997.

Vigneron A, Roninson IB, Gamelin E and Coqueret O (2005) Src inhibits adriamycin-induced senescence and G2 checkpoint arrest by blocking the induction of p21waf1. *Cancer Res* **65**(19):8927-8935.

Wong RP, Tsang WP, Chau PY, Co NN, Tsang TY and Kwok TT (2007) p53-R273H gains new function in induction of drug resistance through down-regulation of procaspase-3. *Mol Cancer Ther* **6**(3):1054-1061.

Xu HJ, Zhou Y, Ji W, Perng GS, Kruzelock R, Kong CT, Bast RC, Mills GB, Li J and Hu SX (1997) Reexpression of the retinoblastoma protein in tumor cells induces senescence and telomerase inhibition. *Oncogene* **15**(21):2589-2596.

Yuan X, Zhou Y, Casanova E, Chai M, Kiss E, Grone HJ, Schutz G and Grummt I (2005) Genetic inactivation of the transcription factor TIF-IA leads to nucleolar disruption, cell cycle arrest, and p53-mediated apoptosis. *Mol Cell* **19**(1):77-87.

Zhu Y, Poyurovsky MV, Li Y, Biderman L, Stahl J, Jacq X and Prives C (2009) Ribosomal protein S7 is both a regulator and a substrate of MDM2. *Mol Cell* **35**(3):316-326.

Downloaded from molpharm.aspetjournals.org at ASPET Journals on April 18, 2024

Footnotes: This work was supported by NIH grant [5R01-CA064192] to Beverly S. Mitchell and by a SCOR Award [LLS SCOR 7007-09] and translational awards [LLS TRP 6203-11] to Beverly S. Mitchell from the Leukemia and Lymphoma Society.

Downloaded from molpharm.aspetjournals.org at ASPET Journals on April 18, 2024

Molecular Pharmacology Fast Forward. Published on April 4, 2011 as DOI: 10.1124/mol.110.070284
This article has not been copyedited and formatted. The final version may differ from this version.

Figure legends:

Fig. 1. Effect of CPEC on SA-*β*-gal induction in MCF-7 and MDA-MB-231 cells. (A, C) MCF-7 or MDA-MB231 cells were seeded in 12 well plates at a density of 1×10^5 cells/well and continuously exposed to CPEC, 10μM nutlin-3a or vehicle control for five days. Control cells were grown for three days and then passaged. Cells were washed, fixed and stained at pH 6.0 as described in Materials and Methods. **(A)** Comparison of CPEC effects on induction of SA-*β*-gal in MCF-7 and MDA-MB231 cells. Scale bar represents 20.7 μm for control MCF-7 cells; **(B)** Bar graph showing the percentages of β-galactosidase-positive cells (mean ± SD) in five randomly selected fields of MCF-7 cells containing at least 50 cells per field; (C) Comparison of effects of Nutlin-3a on the two cell lines. Scale bar represents 20.7 μm for control MCF-7 cells.

Fig. 2. Effect of cytidine on CPEC-induced senescence and differentiation. MDA-MB-231 **(A)** and MCF-7 **(B)** cells seeded in 12 well plates at a density of 1×10^5 cells/well were pre-incubated with 100 μM cytidine for 30 min. and continuously exposed to increasing concentrations of CPEC or vehicle control for five days in the absence or presence of cytidine. Control cells were allowed to grow for three days and passaged. Cells were washed, fixed and stained for Oil-Red O (MDA-MB-231) or SA-β-gal (MCF-7) as described in Materials and Methods and photographed at 20× magnification. Scale bar represents 20.3 μm for the MDA-MB-231 control cells and 20.7 μm for the MCF-7 cells.

Fig. 3. Differential effects of CPEC on cell cycle progression and BrdU incorporation in MCF-7 cells. Analyses of cell cycle progression (A) and BrdU incorporation (B) in MCF-7 were performed as described in Materials and Methods after 5 days of culture in the absence or presence of CPEC at the concentrations indicated. The percentage of cells in each phases

Downloaded from molpharm.aspetjournals.org at ASPET Journals on April 18, 2024

of the cell cycle is indicated for each sample in the histogram. Yellow circles indicate S phase-arrested cells lacking active BrdU incorporation. Data shown are representative of two experiments.

Fig. 4. Differential effects of CPEC on cell cycle progression and BrdU incorporation in MDA-MB-231 cells. Analyses of cell cycle progression (A) and BrdU incorporation (B) in MDA-MB-231 cells were performed as described in Materials and Methods after 5 days of culture in the absence or presence of CPEC at the concentrations indicated. The percentage of cells in each phases of the cell cycle is indicated for each sample in the histogram. Data are representative of two experiments.

Fig. 5. Differential effects of CPEC on the p53/p21 pathway. Immunoblot analysis of p53, nucleostemin, Mdm2, p21, γ-H2A, and p-γ-H2AX in MCF-7 **(A)** and MDA-MB-231 cells **(B)** in the absence or presence of 1 μM CPEC. Beta-actin serves as a loading control.

Fig. 6. Effect of p53 siRNA on CPEC-induced senescence in MCF-7 cells. MCF-7 cells were transfected with 100 nM/200 nM p53-siRNA or control-siRNA by Amaxa electroporation. **(A)** Twenty-four hours post-transfection, the cells were treated with 1 μM CPEC for 20 h, and 40 μg of cell lysate were subjected to western blot analysis using antibodies against p53, Mdm2, p-γ-H2AX, and γ-H2A. Beta-actin served as loading control; **(B)** 5 days after CPEC treatment, the cells were stained for β-gal activity. Cells were photographed at ×20 magnification. Scale bar represents 20.3 μm for control MCF-7 cells. **(C)** Bar graph showing the percentage of β-galactosidase-positive cells (mean ± SD) counted in five randomly selected fields containing at least 50 cells per field. **(D)** 24 h after Amaxa electroporation of 100 nM p53-siRNA or control-siRNA, the cells were treated with 1 μM CPEC for five days, and then stained with Annexin-V and PI followed by flow cytometric analysis. **(E)** HL60 cells were treated with CPEC at doses indicated for 32 h, and then stained

Downloaded from molpharm.aspetjournals.org at ASPET Journals on April 18, 2024

Molecular Pharmacology Fast Forward. Published on April 4, 2011 as DOI: 10.1124/mol.110.070284
This article has not been copyedited and formatted. The final version may differ from this version.

with Annexin-V and PI followed by flow cytometric analysis.

Fig. 7. Effect of CPEC on the localization of the nucleolar proteins nucleostemin, Mdm2, and nucleolin in MCF-7, MDA-MB-231 cells, and U2OS cells. (A) MCF cells and (B)MDA-MB-231 cells were treated with 1 μM CPEC for 8 h. Cells were then fixed, permeabilized, and stained for NS and Mdm2 as described in Materials and Methods and photographed using fluorescent microscopy at ×100 magnification. (**C**) U2OS cells were treated with 1 μM CPEC for 8 h, fixed, permeabilized, stained for NS and nucleolin, and photographed using fluorescent microscopy at 100x magnification.

Downloaded from molpharm.aspetjournals.org at ASPET Journals on April 18, 2024

Fig. 1

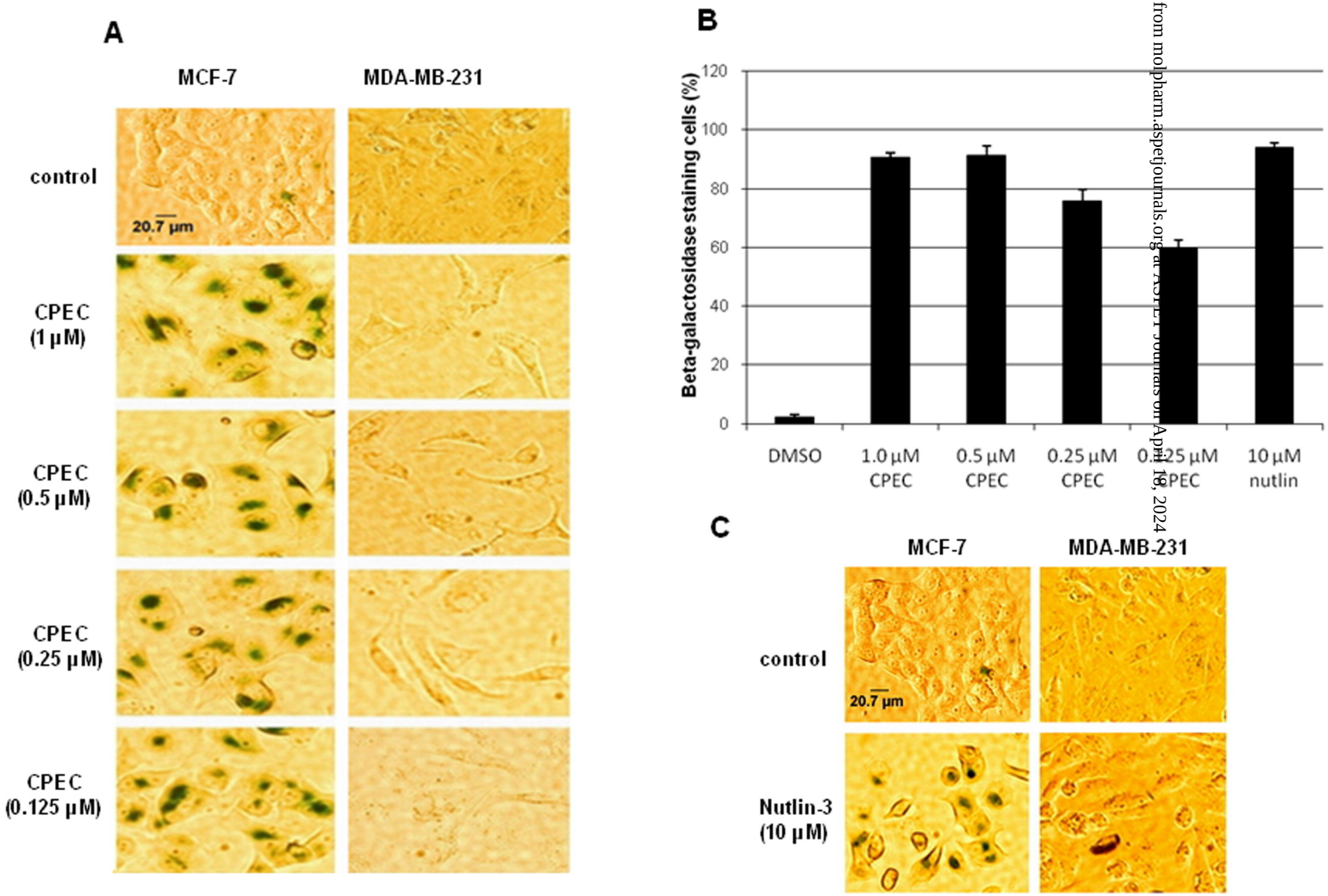

Downloaded from molpharm.aspetjournals.org at ASPET Journals on April 19, 2024

Fig. 2

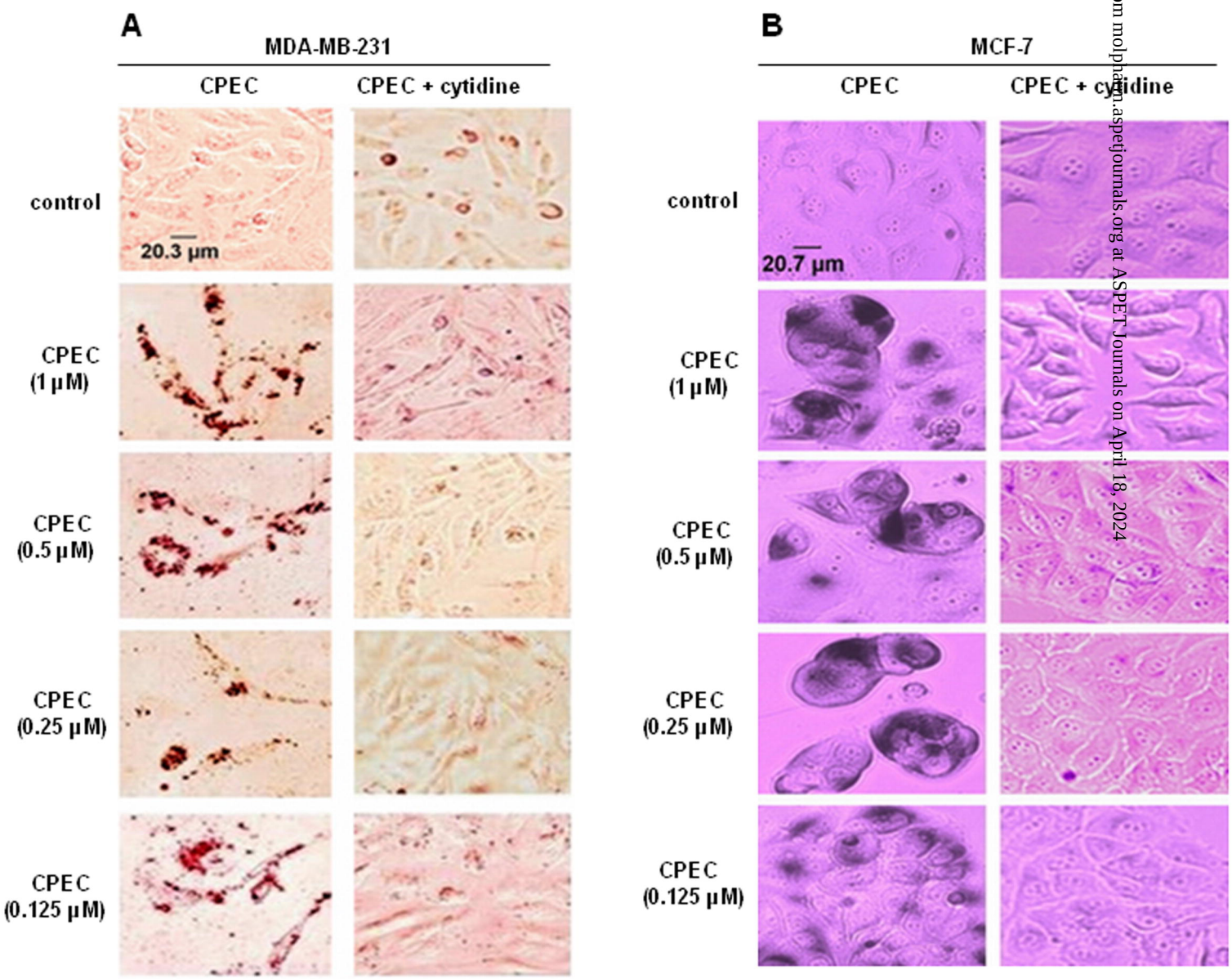

Downloaded from molpharm.aspetjournals.org at ASPET Journals on April 18, 2024

Fig. 3

MCF-7 cells

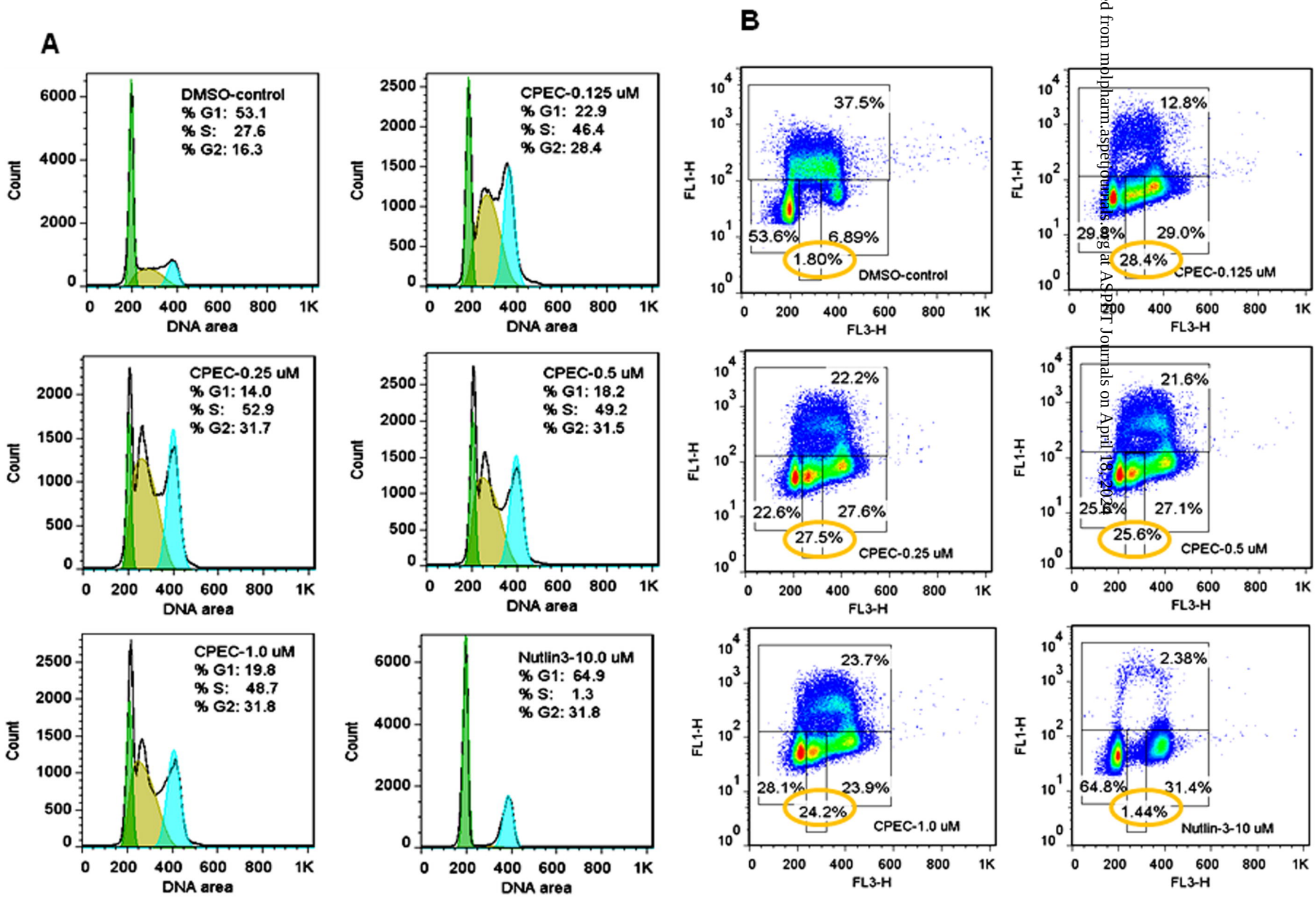

Downloaded from molpharm.aspetjournals.org at ASPET Journals on April 18, 2024

Fig. 4

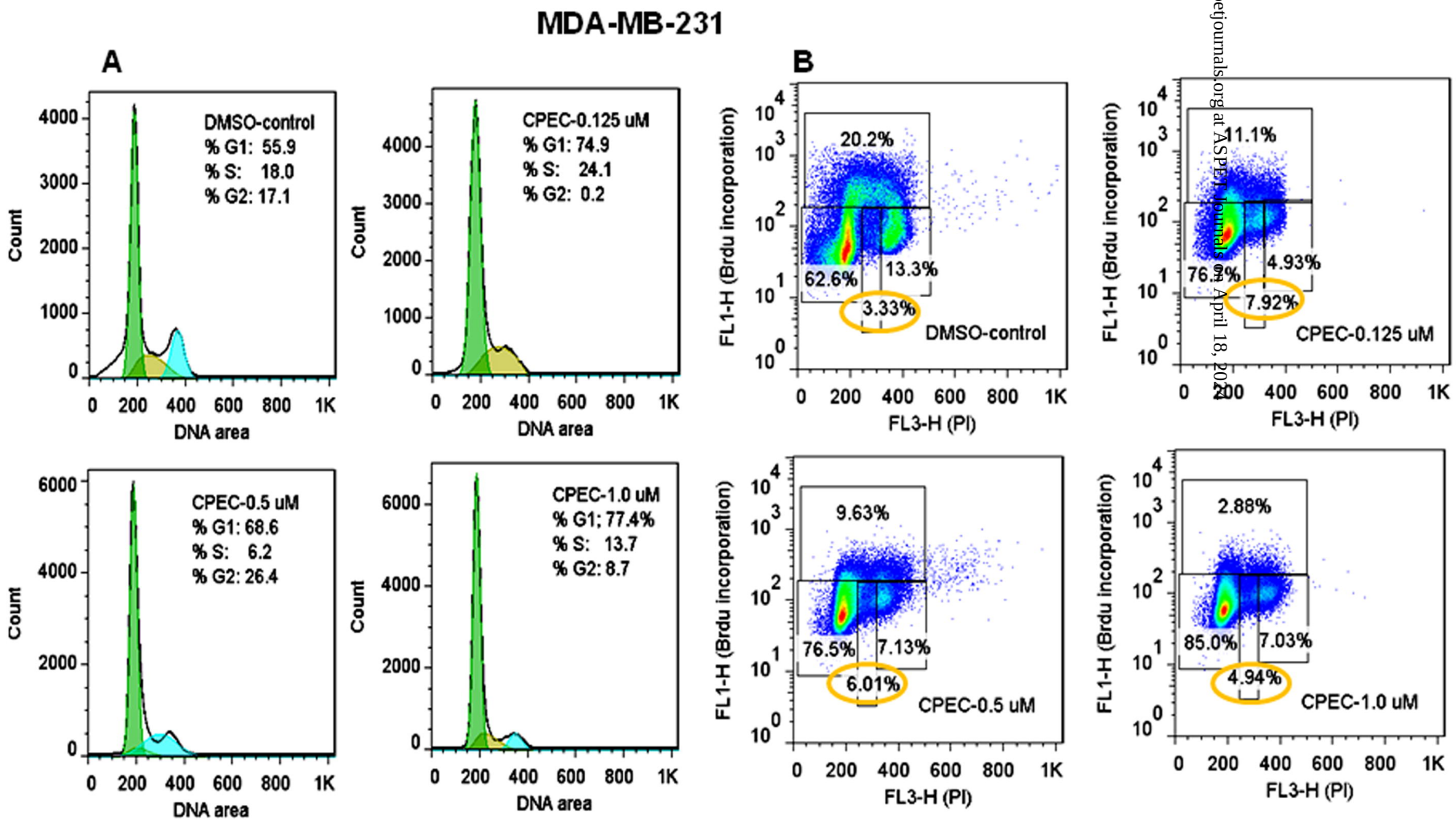

Downloaded from molpharm.aspetjournals.org at ASPET Journals on April 18, 2024

Fig. 5

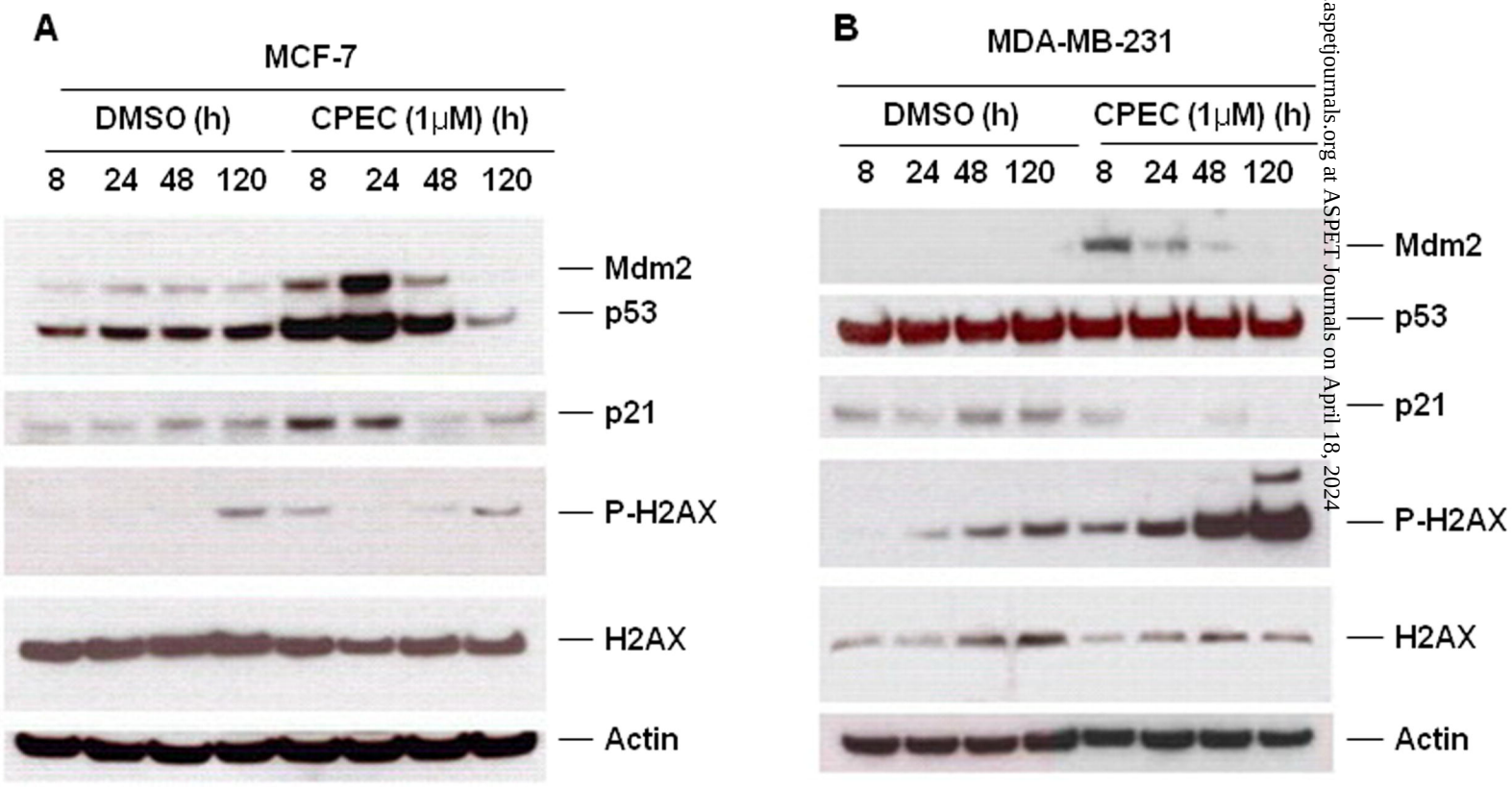

Downloaded from molpharm.aspetjournals.org at ASPET Journals on April 18, 2024

Fig. 6

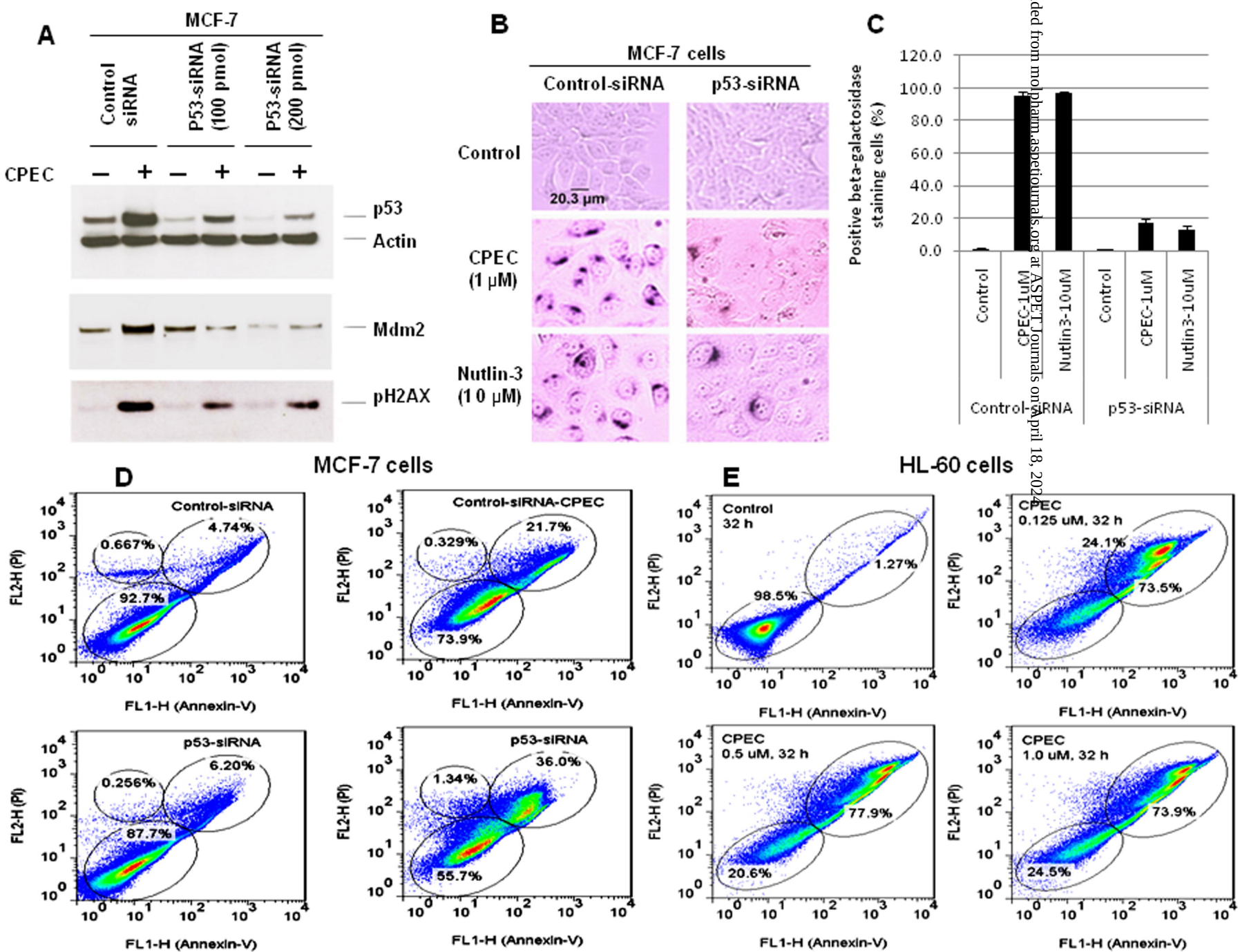

Downloaded from molpharm.aspetjournals.org at ASPET Journals on April 18, 2024

Fig. 7

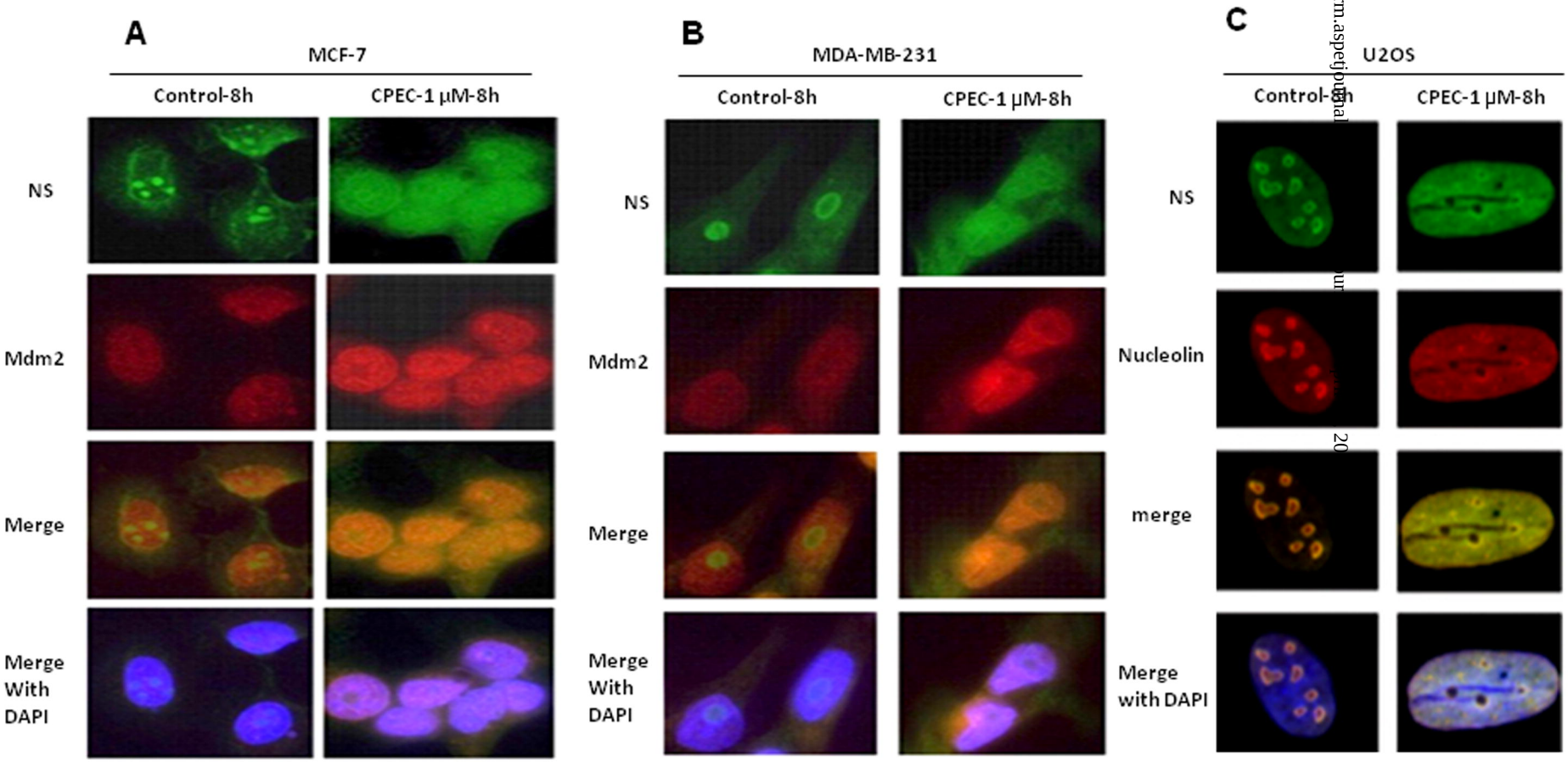

Downloaded from molpharm.aspetjournals.org

Molecular Pharmacology

Cyclopentenyl cytosine induces senescence in breast cancer cells through the nucleolar stress response and activation of p53

Min Huang, Patrick Whang, Patrick Lewicki, and Beverly S. Mitchell

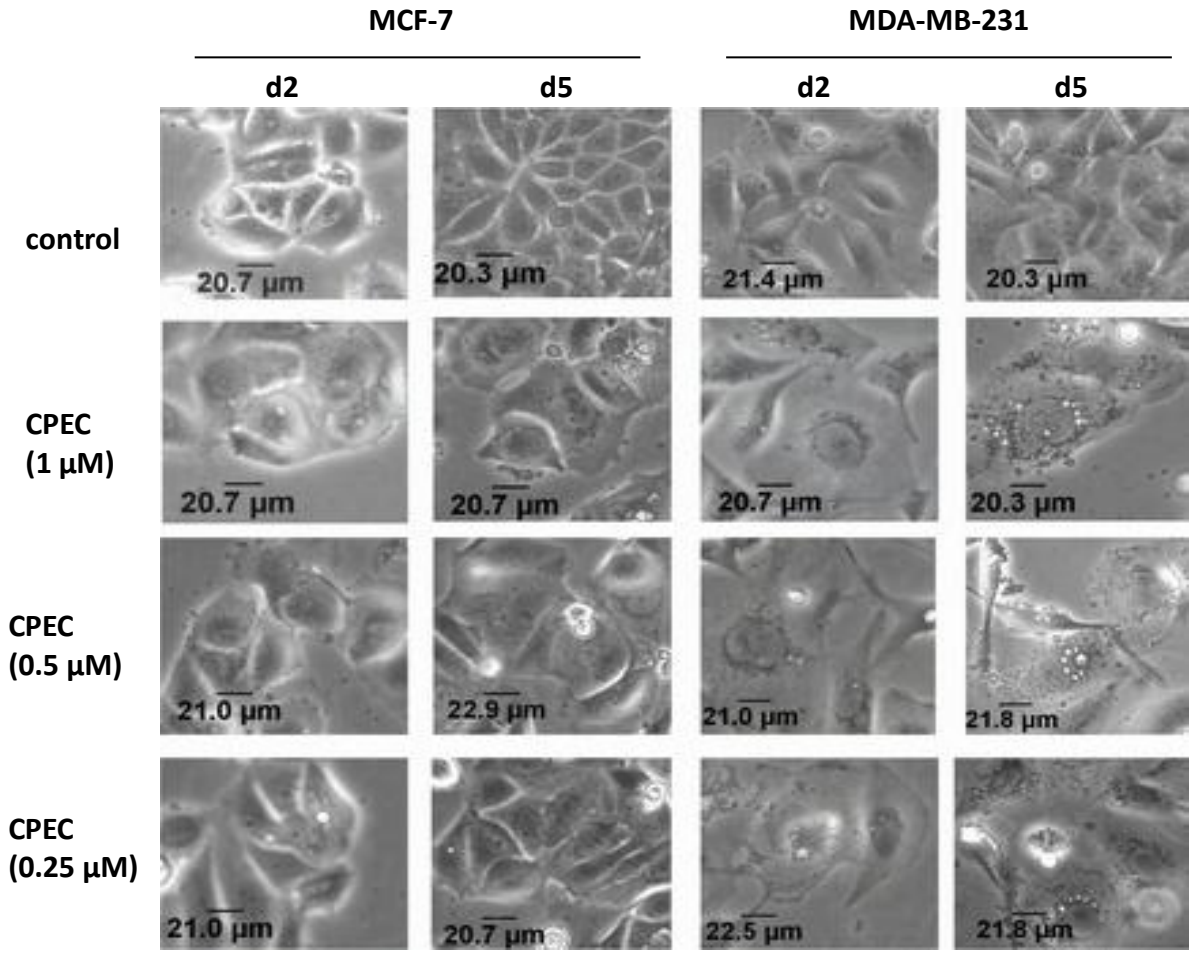

Fig. 1. Induction of morphological changes in MCF-7 and MDA-MB cell lines by CPEC. Cell lines were examined using a Nikon Eclipse TE200 microscope (40×) at days 2 and 5 after the addition of the indicated concentrations of CPEC. Scale bars ranged from 20.3 and 22.9 µm.

Molecular Pharmacology

Cyclopentenyl cytosine induces senescence in breast cancer cells through the nucleolar stress response and activation of p53

Min Huang, Patrick Whang, Patrick Lewicki, and Beverly S. Mitchell

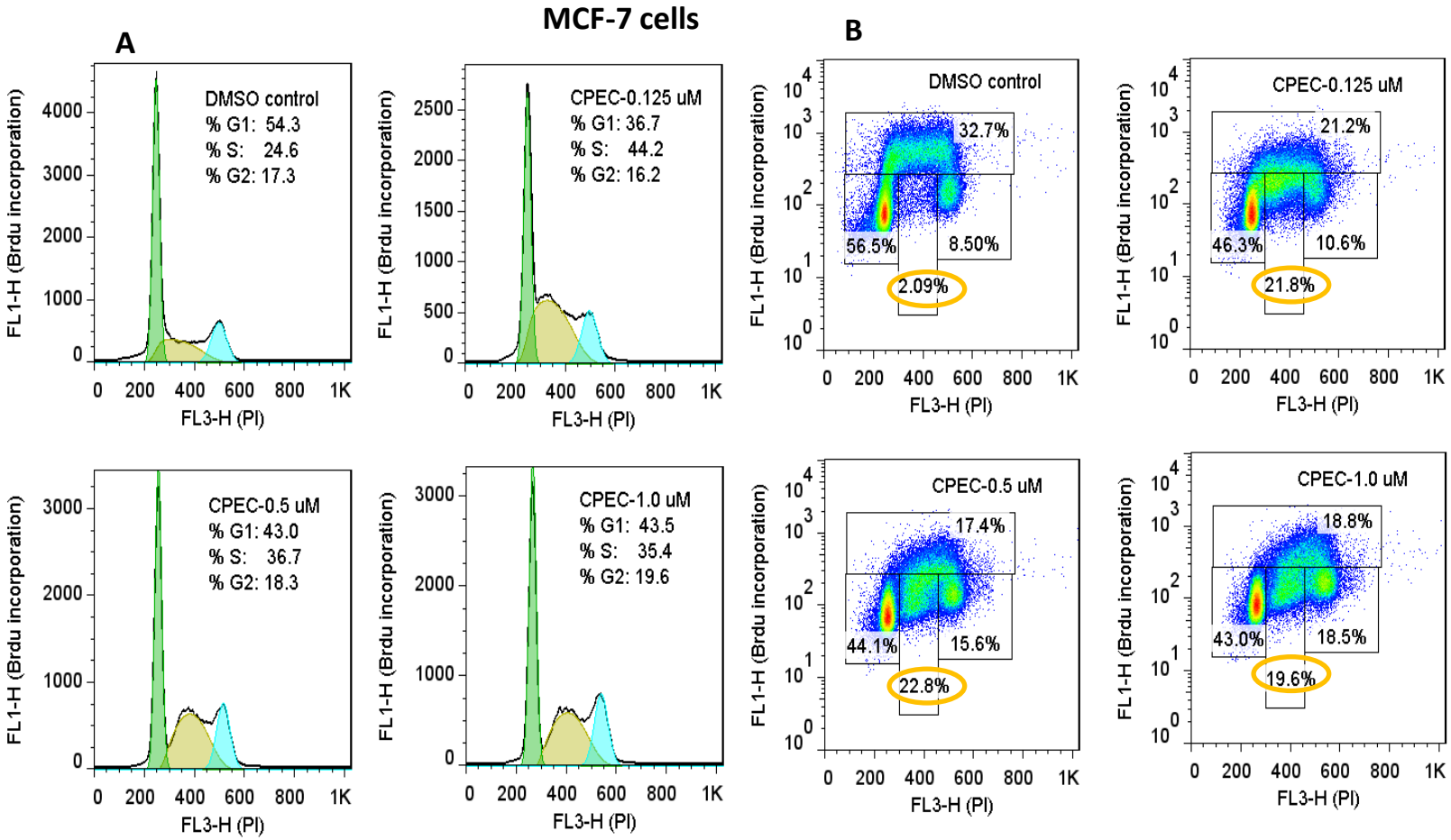

Fig. 2. Differential effects of CPEC on cell cycle progression and BrdU incorporation in MCF-7 cells. Analyses of cell cycle progression (A) and BrdU incorporation (B) in MCF-7 cells were performed as described in Materials and Methods after 48 h of culture in the absence or presence of CPEC at the concentrations indicated. The percentage of cells in each phases of the cell cycle is indicated for each sample in the histogram. Yellow circles represent S phase-arrested cells lacking BrdU incorporation.

Molecular Pharmacology

Cyclopentenyl cytosine induces senescence in breast cancer cells through the nucleolar stress response and activation of p53

Min Huang, Patrick Whang, Patrick Lewicki, and Beverly S. Mitchell

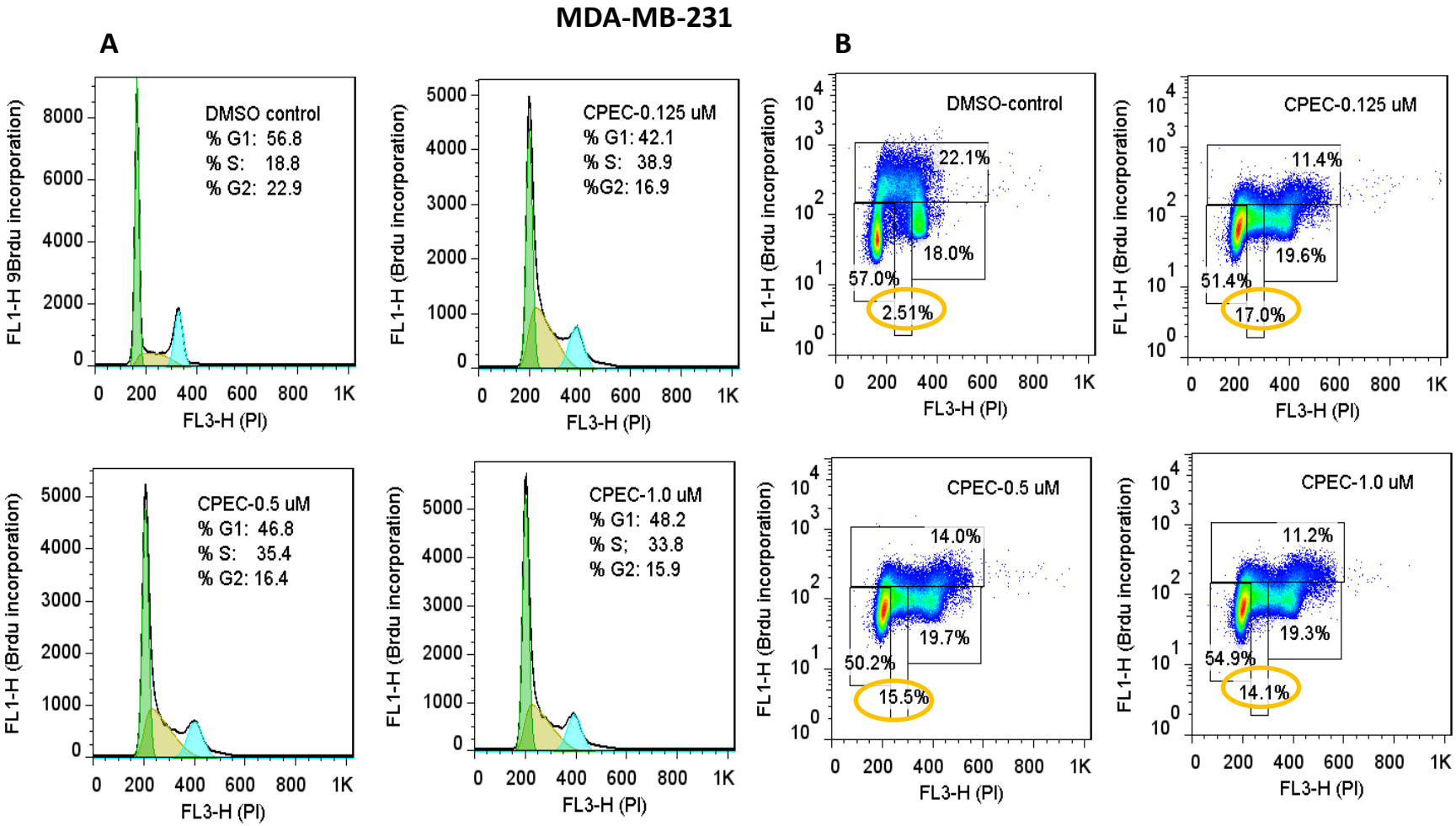

Fig. 3. Differential effects of CPEC on cell cycle progression and BrdU incorporation in MDA-MB-231 cells. Analyses of cell cycle progression (A) and Brdu incorporation (B) in MDA-MB-231 cells were performed after 48 h of culture in the absence or presence of CPEC at the concentrations indicated. The percentage of cells in each phases of the cell cycle is indicated for each sample in the histogram. Yellow circles represent S phase-arrested cells lacking BrdU incorporation.

Molecular Pharmacology

Cyclopentenyl cytosine induces senescence in breast cancer cells through the nucleolar stress response and activation of p53

Min Huang, Patrick Whang, Patrick Lewicki, and Beverly S. Mitchell

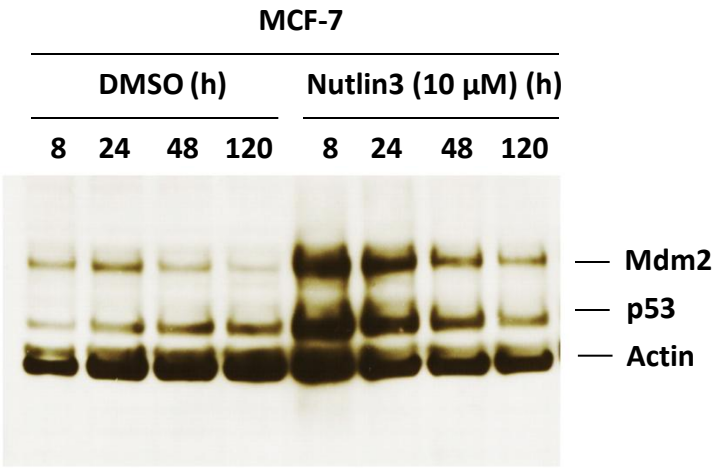

Fig. 4. Induction of p53 and Mdm2 by Nutlin 3 in MCF-7 cells. Immunoblot analysis of p53 and Mdm2 was performed in MCF-7 cells in the presence or absence of 10 µM Nutlin 3 for the time indicated. Beta-Actin was used as a loading control.

Cyclopentenyl cytosine induces senescence in breast cancer cells through the nucleolar stress response and activation of p53

Min Huang, Patrick Whang, Patrick Lewicki, and Beverly S. Mitchell

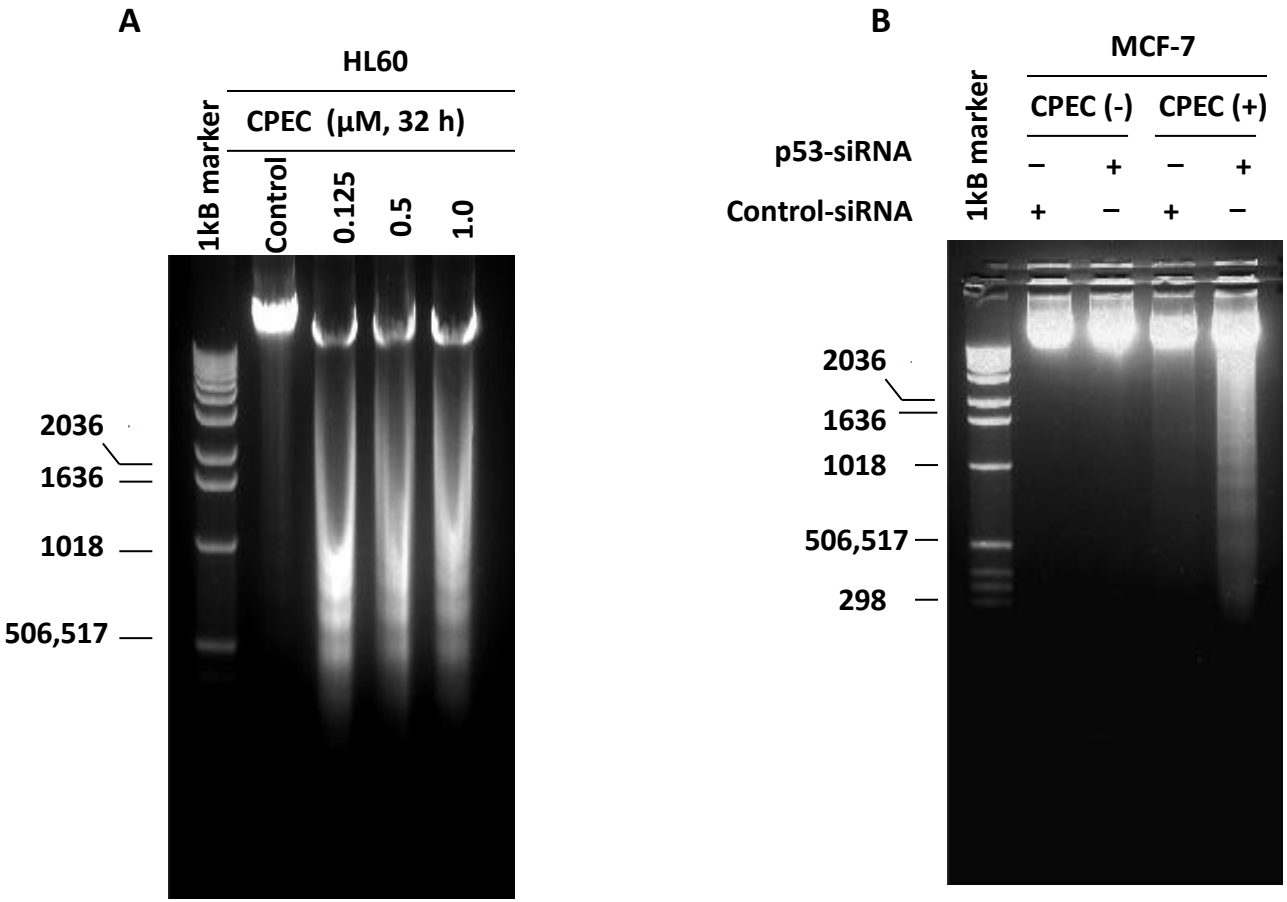

Fig. 5. Induction of DNA fragmentation by CPEC and effect of p53 depletion. (**A**) HL60 cells were treated with CPEC or control vehicle at doses indicated for 32 h. The DNA extracted was separated using agarose gel electrophoresis. Lane 1: 1 kB DNA marker; lane 2, HL60 cells: control; lane 3, HL60 cells: CPEC-0.125 µM, 32 h; lane 4, HL60 cells: CPEC-0.5 µM; Lane 5, HL60 cells: CPEC-0.5 µM. (**B**) MCF-7 cells were transfected with 100 nM p53-siRNA or control-siRNA by Amaxa electroporation. Twenty-four hours post-transfection, the cells were treated with 1 µM CPEC for five days prior to DNA extraction. Lane 1: 1kB DNA marker; lane 2: control-siRNA; lane 3: p53-siRNA; lane 4: control-siRNA +CPEC; Lane 5: p53-siRNA +CPEC.

Cyclopentenyl cytosine induces senescence in breast cancer cells through the nucleolar stress response and activation of p53

Min Huang, Patrick Whang, Patrick Lewicki, and Beverly S. Mitchell

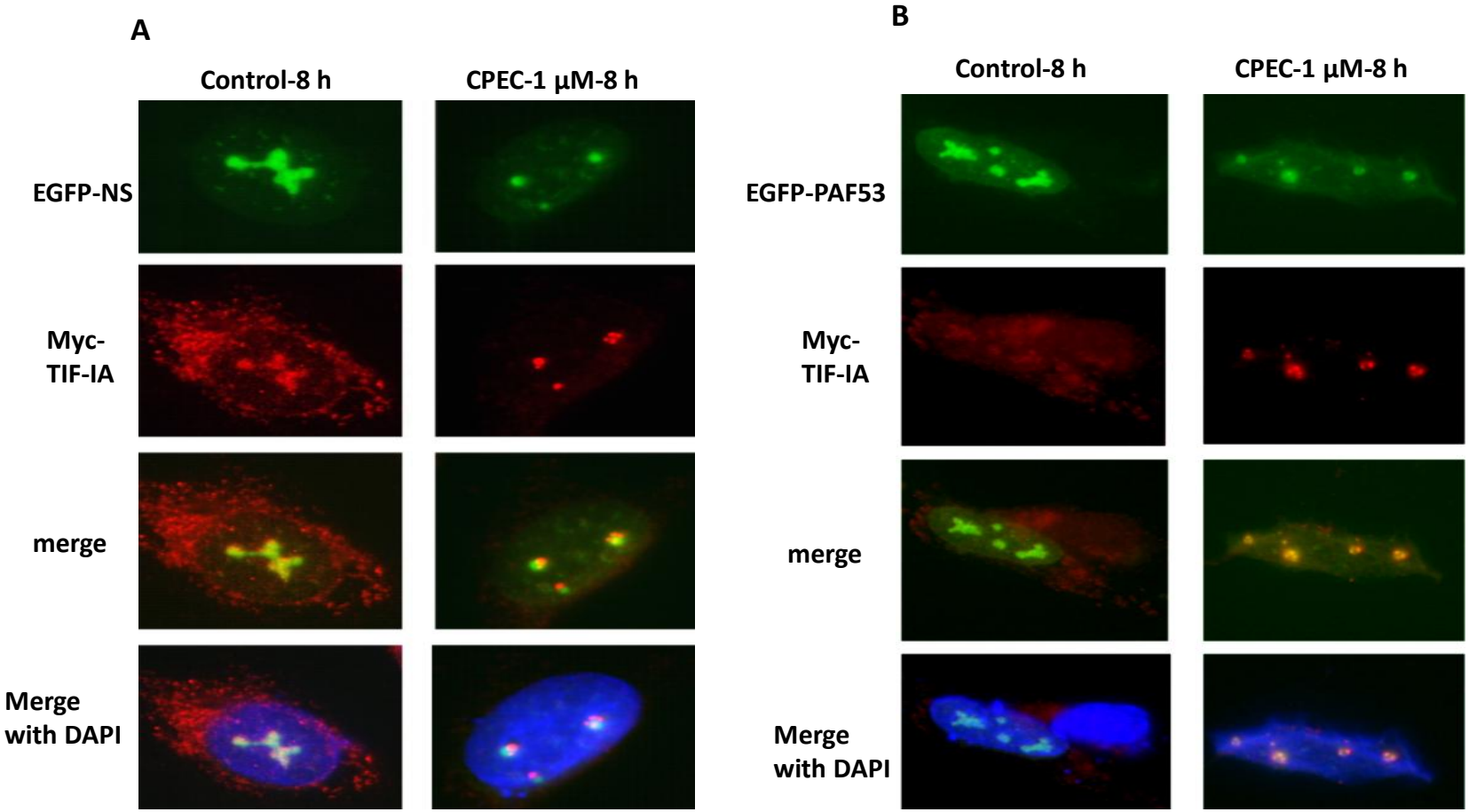

Fig. 6. CPEC-induced translocation of TIF-IA and PAF53 to the nucleolar cap. (A) U2OS cells were co-transfected with EGFP-NS and Myc- TIF-IA or **(B)** with EGFP-PAF53 and Myc-TIF-IA as described previously (Huang et al., 2008). Twenty-four hours post-transfection, cells were treated with 1 µM CPEC for 8 h and observed using fluorescent microscopy at 100× magnification.